ACS OMEGA

http://pubs.acs.org/journal/acsodf

Article

Effect of Alkali and 1,4-Butanediol Contents on the Extraction of Lignin and Lignin-Based Activated Carbon

Ying-xia Li, Shao-xing Hou, Quan-yuan Wei, Xiao-shan Ma, and Yong-Shui Qu*

Cite This: *ACS Omega* 2021, 6, 34386−34394

Read Online

ACCESS | Metrics & More | Article Recommendations

ABSTRACT: In the process of lignin extraction by the organic solvent method, the amount of alkali and the content of 1,4-butanediol are important conditions that affect lignin yield. The effects of alkali and alcohol contents on lignin recovery, removal rate, and structure were studied. In this reaction system, the removal rate of lignin increased with the increase of alkali content but decreased with the increase of alcohol content. Fourier transform infrared (FT-IR) analysis showed that the phenol hydroxyl group and the ether bond in lignin had different trends in different alkali and 1,4-butanediol environments, and four different infrared parameters in lignin had an obvious linear relationship. Gel permeation chromatography (GPC) results showed that high alkali content and high 1,4-butanediol content could lead to the fragmentation of lignin. In addition, lignin extracted from alkali-quantity factor series was selected to prepare activated carbon, $CaCl_2$ was selected as the activator, and its effects were studied. Results showed that in the process of extracting lignin, on the one hand, NaOH content affects the functional groups of activated carbon by affecting the aromatic structure of lignin; on the other hand, the NaOH content affects the graphitization degree and specific surface area of activated carbon by affecting the removal rate and the molecular weight of lignin.

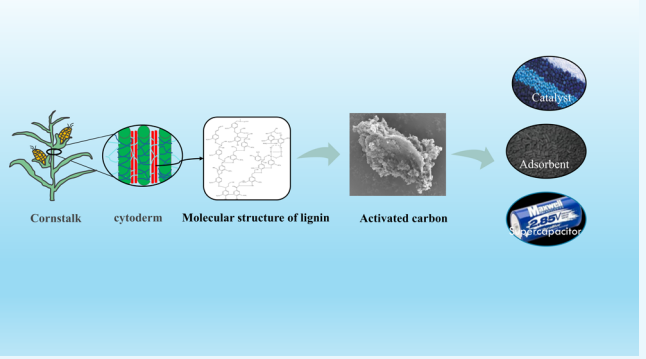

1. INTRODUCTION

Lignin is one of the three components of biomass as a byproduct in the preparation of bioethanol, and pulp has been widely produced and focused on.[1] Lignin is an amorphous compound composed of three monomers, namely, *p*-coumaryl alcohol (H), coniferyl alcohol (G), and sinapyl alcohol (S), which are linked by C−O or C−C.[2] It has great potential for production in phenolic resins, adhesives, and aromatic monomers.[3] However, considering its complex structure and difficulties in extraction and purification, lignin has not been well developed and utilized.[4] The reason the natural structure of lignin depends on the species is that different species have different chemical compositions and monomer ratios. In addition, the isolated lignin has high heterogeneity and low reactivity and purity, which depends on the covalent combination of lignin and carbohydrate to form a lignin carbohydrate complex (LCC). Only 2% of the lignin obtained from the pulp and paper industry is commercially utilized.[1,5,6]

Lignin with a carbon content of 60−65% is an ideal precursor for the preparation of activated carbon. The preparation of carbon materials by carbonization of biomass for adsorption, catalyst carrier, electrode, and energy storage has been widely studied.[7,8] For example, Chang et al. used sodium lignosulfonate obtained from papermaking wastewater to prepare new activated carbon for the adsorption of antibiotics in water, showing good adsorption capacity and regeneration capacity.[9] Klose et al. used a two-step activation method and KOH as the activator to prepare lignin-based polyporous carbon as the active material for supercapacitors.[10] This material has then been considered to carbonize the extracted lignin to obtain activated carbon, which can effectively reduce environmental pollution and the waste of lignin resources in industrial production. Meanwhile, considering the use of cellulose and hemicellulose and the preparation of high-value chemicals (e.g., levulinic acid, glucose, 5-hydroxymethyl furfural), propionate, and biofuels (such as ethanol, butanol, 2-methyl furan),[6] research on carbonization of lignin extracted from stalk can not only make use of the characteristics of lignin but also realize the effective utilization of resources.

Generally, the separation methods of lignin in plant fiber materials can be divided into four categories, namely, solvent

Received: August 11, 2021
Accepted: November 10, 2021
Published: December 6, 2021

https://doi.org/10.1021/acsomega.1c04318
ACS Omega 2021, 6, 34386−34394

fractionation and biological, physical, and chemical methods. Among these extraction methods, the organic solvent method is regarded as the most promising one. Not only does the lignin extracted by the organic solvent have high quality and can be used for the production of various chemicals but also the organic solvent can be recycled through distillation, which is more environmentally friendly.[11] For example, Wang et al. used the organic solvent extraction method to separate lignin and studied the average molecular weight and dispersion of lignin via gel permeation chromatography (GPC) and Fourier transform infrared (FT-IR) and thermal analyses.[12] Zhang et al. used methanol/water as solvent to extract sulfate lignin from eucalyptus wood and proposed the mechanism for color differentiation.[13] In the process of extracting lignin from corn stalk by the organic solvent method, although NaOH has a good effect, it also has the disadvantage of high cost. Therefore, the amount of alkali is selected as a factor for carbonization research to reduce the production cost.[14]

Carbon materials are prepared from lignin mainly via physical and chemical activation. The physical activation method has mild conditions and low requirements for equipment but incurs a long time and high energy consumption. Hence, the chemical activation method is more favored by researchers. The chemical activation method has the characteristics of low reaction temperature, high yield, and simple operation.[15] The main activators used are KOH,[16] NaOH,[17] and $ZnCl_2$.[18] Song et al. designed a new method to prepare activated carbon with a high specific surface area from rice husk using NaOH, showing the potential utilization value of biomass.[19] However, the above activators may cause corrosion of instruments and equipment and increase the cost; hence, low cost, availability, and environmental friendliness of calcium chloride are considered.[20] In the present paper, calcium chloride was used as a catalyst to prepare activated carbon.

In the present paper, the effects of different alkali and 1,4-butanediol contents on the removal and the recovery rate of lignin from corn stalk were studied. The characteristic parameters of lignocellulose were calculated using FT-IR spectroscopy, and the curve of related parameters was fitted. The molecular weight of lignin was analyzed using GPC, and the structure of lignin was studied by the valence bond analysis of lignin. X-ray diffraction (XRD), FT-IR and Raman spectroscopies, and N_2 sorption were used to analyze the influence of alkali content on the structure of lignin-based activated carbon during lignin extraction.

2. MATERIALS AND METHODS

2.1. Materials. Corn stalk raw materials were collected in Changping, Beijing, after natural air-drying, crushed to less than 2 mm, and stored in self-sealed bags for use. The components of corn stalk were 25.95 ± 0.51% cellulose, 27.86 ± 0.71% hemicellulose, 19.66 ± 0.22% lignin, and 9.52 ± 0.36% ash.

2.2. Analytical Methods. *2.2.1. Sample Composition Analysis.* The two-step acid treatment method was used for the analysis of stalk raw materials, lignin, and cellulose components. The monosaccharide content was determined using high-performance liquid chromatography (HPLC).

The experimental procedures are as follows. Briefly, 0.1500−0.1600 g of sample was precisely added into a high-borosilicate test tube, and 1.50 mL of 72% (W/V) concentrated sulfuric acid was added. After shaking and mixing, the sample was placed in a 30 °C water bath for 1 h, and 42 mL of deionized water was added to reduce the concentration of sulfuric acid to 4% (W/V). Then, the tube cover was tightened and placed into the autoclave at 121 °C for a 1 h reaction. The liquid after the reaction was vacuumized and filtered, and the solid lignin residue was separated from the liquid by a filtration crucible. The quality of lignin was measured by drying and ashing. The liquid volume was measured after extraction and filtration, 5.00 mL of the liquid was pipetted out accurately into the 10 mL centrifugal tube, and 0.5000−0.5050 g of $Ba(OH)_2$ shock neutralizing liquid was added. Then, the supernatant was centrifuged and extracted, using high-performance liquid chromatography for monosaccharide analysis, and then the cellulose and hemicellulose quality was calculated. The determination of ash content was carried out by placing 0.1500−0.1600 g of stalk in a crucible and then placing the crucible in a muffle furnace at 575 °C for 4 h. The mass change before and after the calculation gave the ash content in the stalk.

The detection conditions are as follows. Agilent is selected as the liquid chromatographic column. For the column of Hi-Plex-H, a refractive index detector (RID) is used, T is 65 °C, 5 mmol of sulfuric acid is selected as the mobile phase, the speed is set to 0.6 mL min^{-1}, and the injection volume is 2 μL.

Then, the cellulose, hemicellulose, and lignin contents were calculated. Formulae 1 and 2 were used for the calculation method of lignin removal rate and recovery rate.

$$Y_{TR} = 1 - \frac{M_{FC} \times C_{FL}}{M_C \times C_L} \quad (1)$$

$$Y_{HR} = \frac{M_{FL} \times P_{FL}}{M_C \times C_L} \quad (2)$$

Y_{TR} is the lignin removal rate, M_{FC} is the mass amount of holocellulose after lignin removal, C_{FL} is the lignin content in holocellulose, M_C is the mass amount of corn stalk raw materials, C_L is the lignin content in raw materials, Y_{HR} is the lignin recovery rate, M_{FL} is the extracted lignin mass amount, and P_{FL} is the extracted lignin purity.

2.2.2. Molecular Weight Analysis. A 100 mg lignin sample was dissolved in 2% NaOH solution and diluted 10 times in 0.1 mol L^{-1} NaAc solution. After filtration with a pore size of 0.45 μm, the molecular weight was determined using gel permeation chromatography. GPC analysis was carried out with Agilent1260 series equipped with RID and a diode array detector. The chromatographic column was TSKgelG-3000PWxl (300 × 7.8 mm^2). The mobile phase was 0.1 M NaAc with a flow rate of 0.6 mL min^{-1}. The temperature of the column temperature box was 35 °C.

2.2.3. Fourier Transform Infrared (FT-IR) Spectroscopy Analysis. A 0.002 g lignin sample was mixed with KBr in an agate mortar in the proportion of lignin/KBr = 1:100 w/w. The functional groups of lignin were measured using an FT/IR-600 plus spectrometer (JASCO Corp., Tokyo, Japan). The average scanning time was 32, the scanning wavelength range was 400−4000 cm^{-1}, and the resolution was 1 cm^{-1}.

2.2.4. XRD Analysis. The instrument model used was D/MAX2500/PC. The X-ray diffraction pattern of the sample was obtained to analyze the composition and the crystal type of the sample.

2.2.5. Raman Spectroscopy Analysis. A Labram800 Raman spectrometer was used to analyze the degree of order and

https://doi.org/10.1021/acsomega.1c04318
ACS Omega 2021, 6, 34386−34394

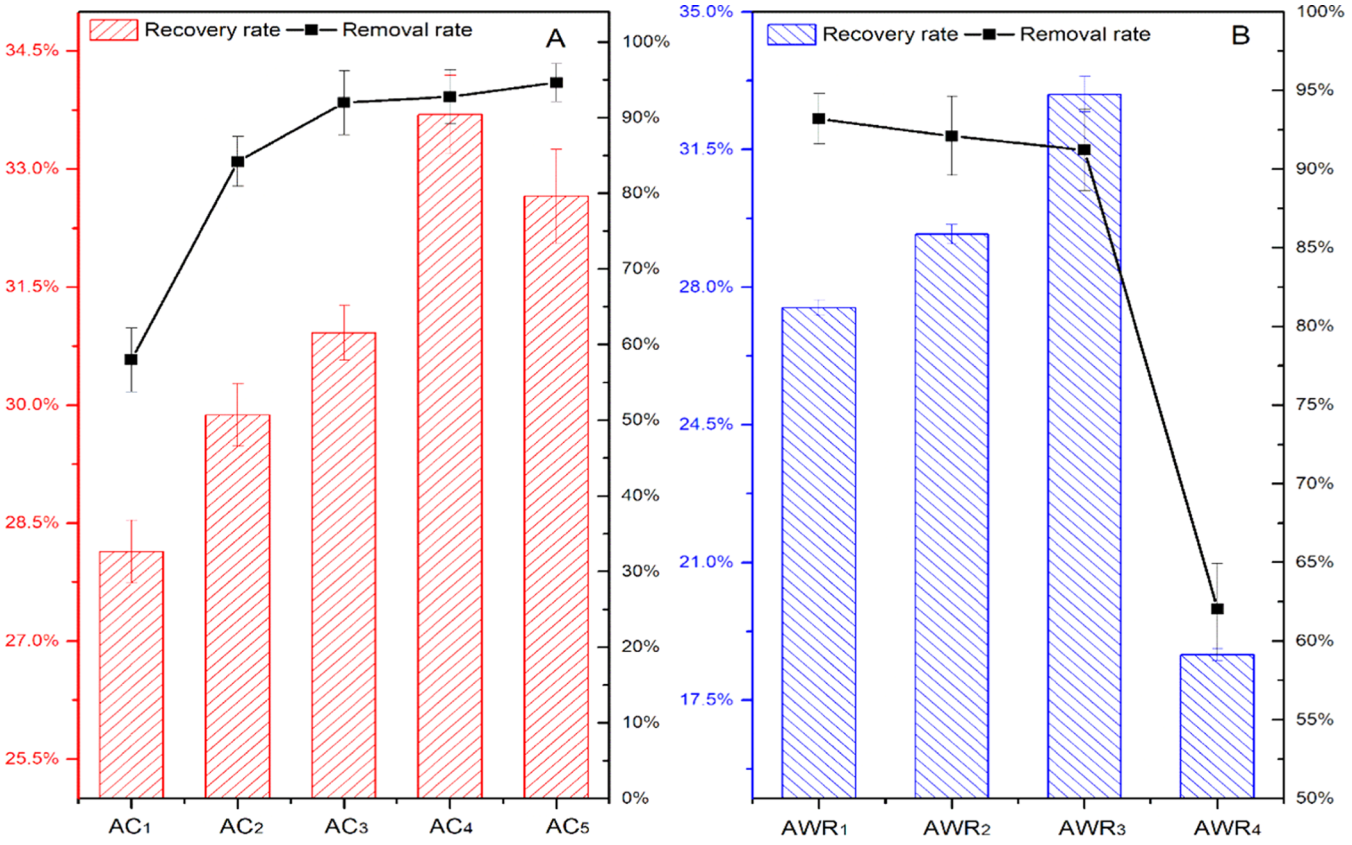

Figure 1. Effect of different alkali and 1,4-butanediol contents on lignin removal and recovery rate. ((A) Solid−liquid ratio, 1:10; 60% 1,4-butanediol; and reaction time, 1 h and (B) solid−liquid ratio, 1:10; NaOH 8 g/stalk 50 g; and reaction time, 1 h.).

defect of activated carbon materials using a 532 nm incident laser.

2.2.6. N_2 Adsorption and Desorption Analysis. Nitrogen adsorption/desorption measurements were performed using an ASAP2460 system (Micromeritics). All samples were degassed at 300 °C for 2 h prior to sorption measurements.

3. RESULTS AND DISCUSSION

3.1. Effect of NaOH and 1,4-Butanediol Contents on Lignin Removal and Recovery Rate. The recovery rate and removal rate of corn stalk lignin are shown in Figure 1. In Figure 1A, with the increase of NaOH content, the removal rate of lignin in corn stalk increased. When the NaOH content was AC_1, the removal rate of lignin was 57.97 ± 4.21%; when the alkali content increased to AC_5, the removal rate increased to 94.66 ± 2.55%. In the reaction, NaOH destroyed the C−O single bond in corn stalk lignin. With the increase of alkali content, the content of free nucleophilic group OH^- in the system increased, thus breaking more C−O single bonds and increasing the lignin removal rate.[21,22] With the increase of NaOH content, the recovery of lignin increases first and then decreases because when the amount of alkali increases, the degree of lignin fracture increases, more lignin is dissolved in the solvent, and the recovery of lignin increases. However, when the amount of alkali exceeded AC_4, a large number of lignin fragments was observed in the solvent, which increased the possibility of reaggregation. Moreover, when the alkali content increased, more sodium lignans were generated (Figure 4D shows that the ash content in lignin increases with the increase of alkali content), which increases the water solubility of lignin, resulting in more lignin dissolving in water and reducing the recovery rate of lignin.

Figure 1B shows that the removal rate of lignin decreases with the increase of 1,4-butanediol content. In the range of AWR_1−AWR_3, the lignin removal rate decreased from 88.32 ± 1.65% to 86.65 ± 3.51%, showing a slight downward trend. With the increase of 1,4-butanediol content in the reaction system, the free OH^- in the system was reduced, the contact chance between the nucleophilic group and lignin was reduced, and the lignin removal rate decreased. Moreover, the increase of 1,4-butanediol content increased the viscosity of the solvent system, which is not conducive to the reaction. In comparison with the removal rate of lignin, the recovery rate of lignin increased first and then decreased. The organic solvent can dissolve the broken lignin, which is beneficial for its separation from the stalk. However, when 1,4-butanediol content was very high, the precipitation of lignin was negatively affected, resulting in a large amount of lignin being dissolved in 1,4-butanediol that cannot be recovered by precipitation.

3.2. Molecular Weight Distribution of Lignin. The weight average relative molecular mass (M_w), number average relative molecular mass (Mn) of lignin, and the calculated polydispersity coefficient D ($D = M_w/M_n$) are shown in Table 1. The molecular weight and the polydispersity coefficient of lignin decreased with the increase of NaOH content. The degradation of lignin was obvious, Mn decreased from 7563 to 4586, and the M_w and the polydispersity coefficient D decreased. With the increase of alkali content, lignin can be further degraded into aromatic substances with small molecules, and the steric hindrance can be reduced, which is conducive to further processing and utilization. Figure 2A

https://doi.org/10.1021/acsomega.1c04318
ACS Omega 2021, 6, 34386−34394

Table 1. Number Average Molecular Weight, Weight Average Molecular Weight, and the Polydispersity Coefficient of Lignin

sample	no. average molecular weight ($g \cdot mol^{-1}$)	molecular weight ($g \cdot mol^{-1}$)	polydispersity coefficient
AC_1	4078	7563	1.85
AC_2	4398	7014	1.59
AC_3	3535	5539	1.57
AC_4	3141	4834	1.54
AC_5	3500	4586	1.31
AWR_1	4100	6489	1.58
AWR_2	3683	5687	1.54
AWR_3	3349	5362	1.60

shows that with an increase of alkali content, lignin fragmentation was intensified, and the lignin content of different fragmentation degrees increased. When the content of 1,4-butanediol increased, the breaking degree of lignin increased, and the molecular weight decreased. Figure 2B shows that when the content of 1,4-butanediol was AWR_4, the peak of lignin at the molecular weight of 1647 was the highest, and the peak of the other molecular weights decreased. Hence, the higher the content of 1,4-butanediol, the easier for the lignin to become a small-molecule compound.

3.3 FT-IR Analysis of Lignin. The absorption peak at 1597 cm^{-1} was used as the internal standard absorption peak, the absorption intensity of the internal standard absorption peak was 100%, and the ratio of other absorption peaks and the internal standard absorption peak was the relative absorption intensity of the absorption peak.[5,23] The characteristic absorption peak of the phenol hydroxyl group of lignin was observed at 1375 cm^{-1} and that of ether bond vibration was observed at 1116 cm^{-1}. Figure 3A shows that with the increase of NaOH content, the relative absorption strength of the ether bond in lignin decreased whereas that of the phenolic hydroxyl group increased. It can be inferred that in the alkaline system of lignin, OH^- breaks the ether bond between lignin, resulting in a decrease of the relative absorption strength of the ether bond. Subsequently, lignin exposed more phenolic hydroxyl groups, resulting in the increase of the relative absorption strength of the phenolic hydroxyl group.

However, in Figure 3B, the trend of phenolic hydroxyl and ether bond changes is positively correlated. With the increase of 1,4-butanediol content in the system, the relative absorption strength of the ether bond and phenolic hydroxyl decreased. Hence, in the reaction system with high 1,4-butanediol content, the C−O single bond of lignin can be broken, but it easily forms sodium lignosulphonate (C−ONa). Based on the composition analysis of lignin in Figure 4C, with the increase of 1,4-butanediol consumption, the ash content in lignin increased because of the formation of more lignin sodium salt in the high 1,4-butanediol reaction system. Lignin can be used to prepare polymer materials such as adhesives, foams, and films because the aromatic side chain of lignin is rich in oxygen-containing groups, such as hydroxyl and methoxy. These active groups are very important for the modification of lignin. Hence, the degradation reaction of lignin should be carried out in a system with low 1,4-butanediol content to prepare highly active lignin materials.

In addition, among the four infrared parameters of lignin, S/G and CLL, L/C, and LOI have an obvious linear correlation trend. The S/G ratio was calculated using A1329/A1328 cm^{-1}, which represents the ratio of the S group and the G group in lignin.[24] CLL was calculated using A1508/A1600 cm^{-1}, which is related to the proportion of condensed lignin and the cross-linking structure.[25] Figure 4A shows that CLL and S/G have a negative linear trend, that is, the larger the S/G, the smaller the CLL value. Based on the structure of the three kinds of lignin

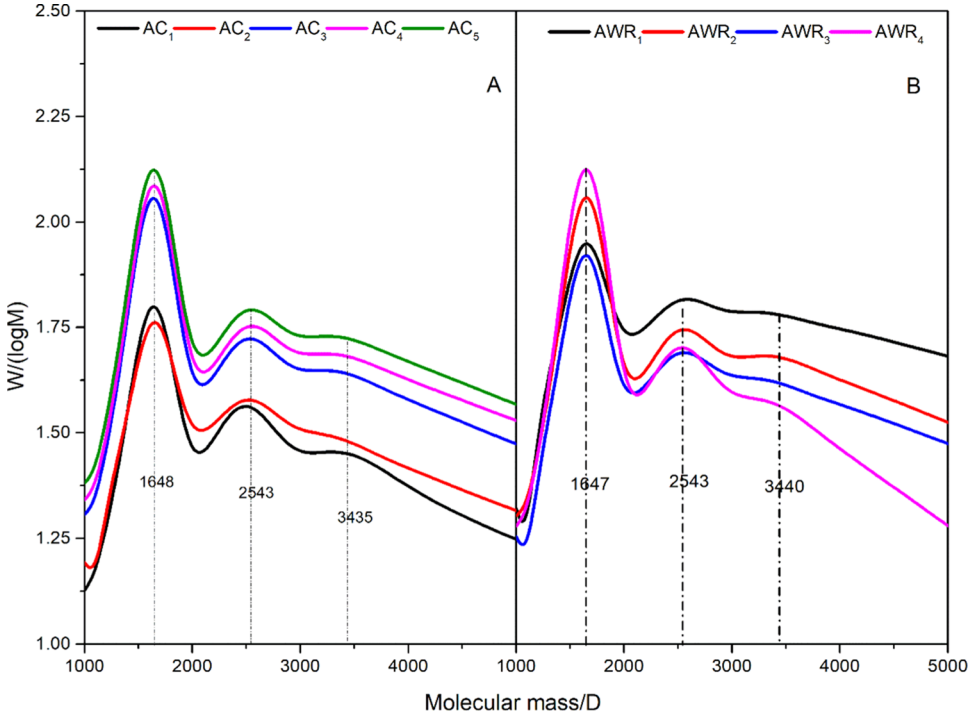

Figure 2. Molecular weight distribution of lignin. (Molecular weight distribution of lignin extracted by different (A) alkali treatments and (B) 1,4-butanediol treatments.).

https://doi.org/10.1021/acsomega.1c04318
ACS Omega 2021, 6, 34386−34394

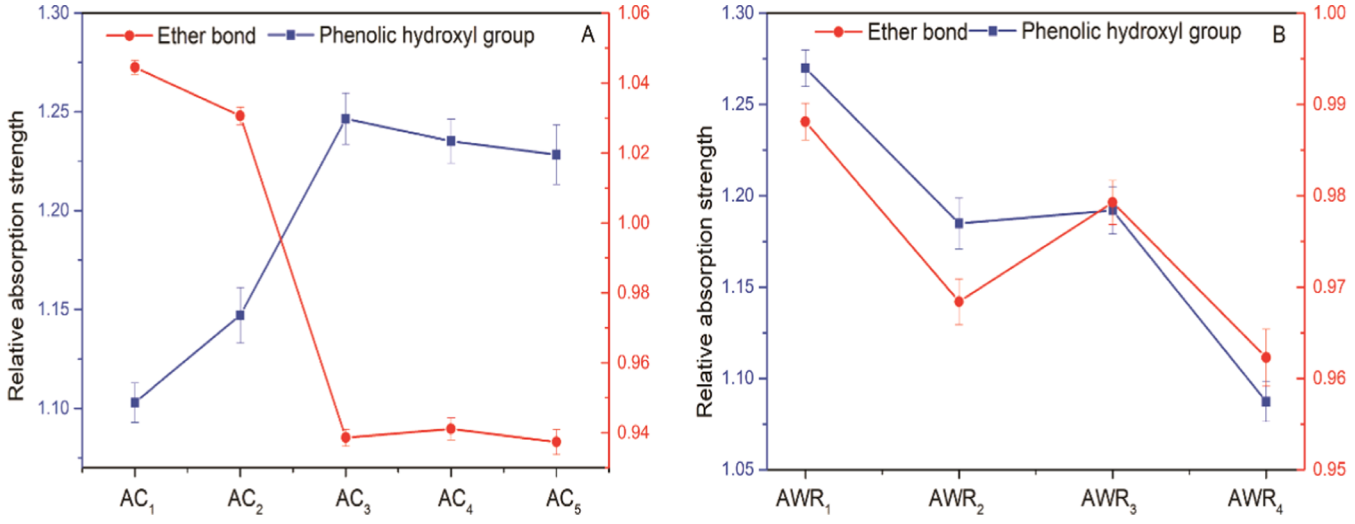

Figure 3. Change trend of ether bond and phenolic hydroxyl in lignin. (Lignin from stalk treated with different (A) alkali contents and (B) 1,4-butanediol contents.).

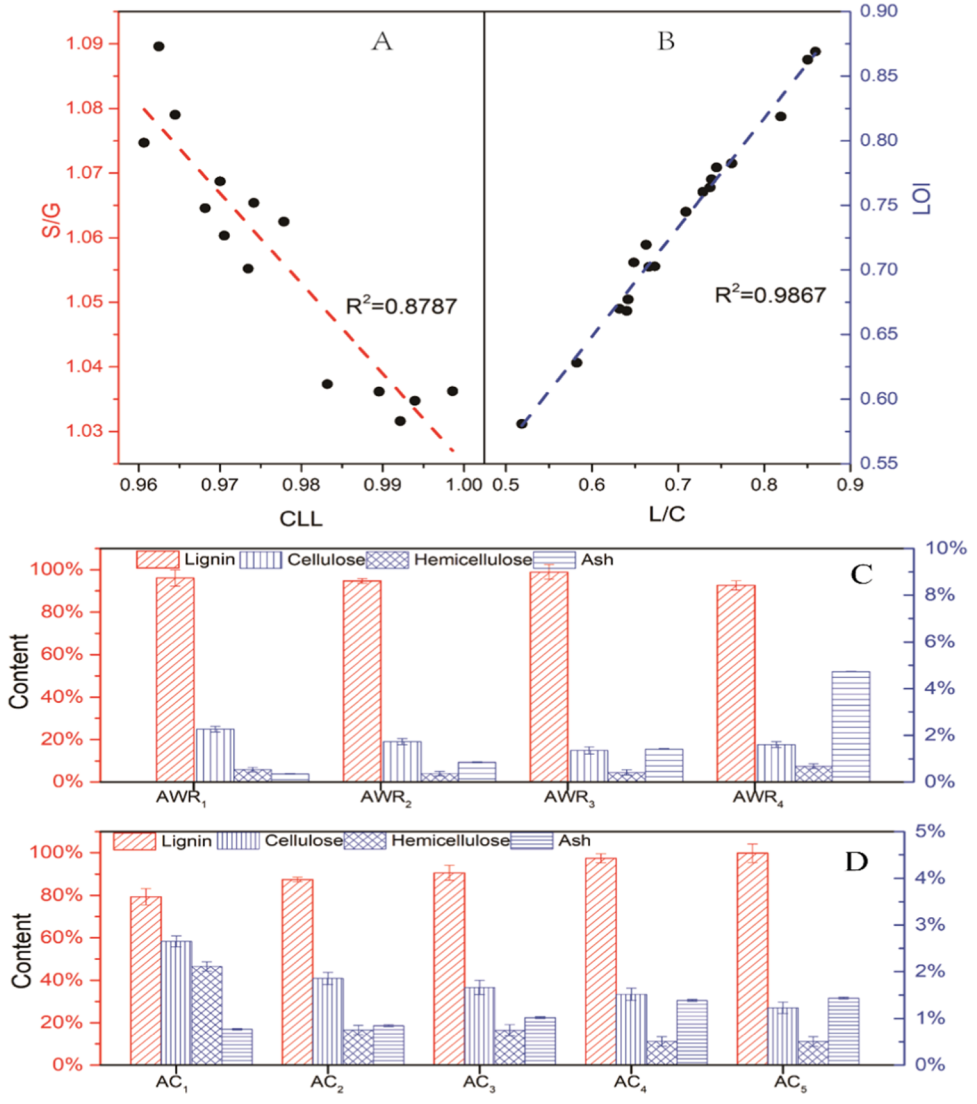

Figure 4. Four infrared characteristic parameters and lignin components. ((A) Fitting diagram of S/G and CLL, (B) fitting diagram of L/C and LOI, (C) lignin components after different 1,4-butanediol treatments, and (D) lignin components after different alkali treatments.).

https://doi.org/10.1021/acsomega.1c04318
ACS Omega 2021, 6, 34386−34394

monomers, a methoxy group was observed at positions 3 and 5 in the benzene ring of the lignin S monomer, and this configuration is conducive to the formation of ether bonds between lignin, further forming the complex three-dimensional structure of lignin. However, the larger the S/G value, the smaller the degree of lignin cross-linking. Hence, the effect of the C−C single bond on the complex structure of lignin is greater than that of the C−O single bond.

The L/C ratio is equivalent to A1508 cm^{-1} (spectrum band of lignin deformation in CH_2 and CH_3)/A900 cm^{-1} (spectrum band of the cellulose amorphous region);[26] the LOI is equivalent to A1430 cm^{-1} (related to the amount of cellulose crystalline structure)/A900 cm^{-1} (the amorphous region of cellulose).[27] Figure 4B shows that LOI is positively correlated with L/C, in which the larger the LOI value, the greater the L/C value. Based on the definition of parameters, both denominators are the infrared absorption intensity of the amorphous area of cellulose. Hence, the positive correlation between them indicates that the higher the purity of lignin, the higher the degree of crystallization of cellulose remaining in lignin. As shown in Figure 4D, with the increase of NaOH content, the purity of lignin increases and the content of hemicellulose and cellulose decreases. However, hemicellulose and cellulose remained in lignin, indicating the presence of LCC in lignin; in addition, lignin, cellulose, and hemicellulose may depend on stable C−C bond connection.

3.4. Characterization of Activated Carbon from Lignin. According to previous studies on biomass-derived carbon, the choice of raw materials mainly affects the properties of activated carbon, which may affect the molecular structure, ash content, and carbon content of activated carbon.[28] To study the effect of lignin structure on the performance of activated carbon rather than the effect of the carbonization process, we prepared activated carbon samples C_1−C_5 from lignin AC_1−AC_5 using the same carbonization method. The reasons for choosing calcium chloride as an activator are as follows: (1) $CaCl_2$ activation method can reduce carbonization and the activation temperature, (2) $CaCl_2$ has a flame retardant effect and can improve the yield of activated carbon, and (3) $CaCl_2$ is cheap and recyclable, which reduces the production cost of activated carbon.[29]

According to the analysis of XRD spectra of lignin-based activated carbon, the XRD spectra have a strong peak located at 23° and a weak peak at 43°, which correspond to the lattice plane (002, 100) without other heteropeaks. The existence of two peaks indicates that the prepared carbon is graphite carbon, and the wide peak indicates amorphous carbon (Figure 5).

FT-IR spectra were widely applied to further study the functional groups of samples. All of the samples displayed similar FT-IR peaks. According to the infrared spectrum analysis of lignin-based activated carbon in Figure 6, the absorption peak near 3407 cm^{-1} in the spectrum is attributed to the stretching vibration of the O−H bond. The absorption peak at 1164 cm^{-1} is attributed to the stretching vibration of the C−O bond. The formation of the aromatic structure in the carbonization process of lignin can be determined from the existence of skeleton vibration, such as (C=C) vibration in the ranges of 1600−1597 and 1597−1392 cm^{-1} and the (C−H) out-of-plane bending vibration in the range of 900−675 cm^{-1}.[30] The higher the alkali content, the further the decomposition of AC_1−AC_4 lignin into small aromatic compounds. Moreover, the higher the S/G value of the

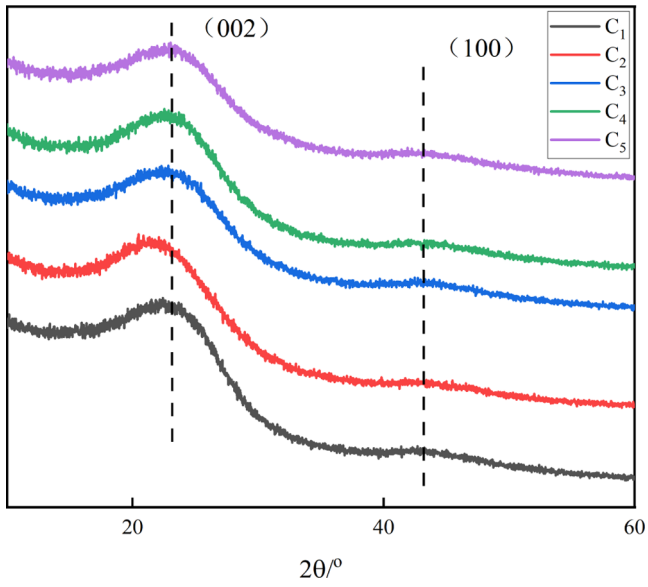

Figure 5. XRD pattern of lignin-based activated carbon.

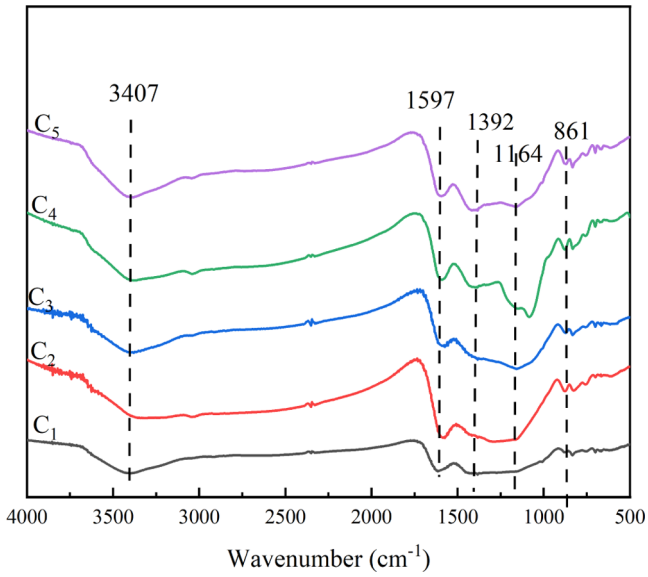

Figure 6. FT-IR spectra of lignin-based activated carbon.

corresponding aromatic compounds, the higher the intensity of C_1−C_4 peaks in the infrared spectrum. The intensity of each absorption peak of C_1 is weak, indicating that the lesser the amount of sodium hydroxide, the lesser the number of oxygen-containing functional groups on the surface, which is not conducive to the adsorption of activated carbon. With the increase of alkali content, the phenolic hydroxyl absorption peak became stronger, and this condition is well correlated with the increase of NaOH content in lignin AC_1−AC_5 to produce more phenolic hydroxyl.

The Raman spectra of lignin-based activated carbon showed two characteristic peaks, namely, D and G peaks, which were located at approximately 1350 and 1580 cm^{-1}, respectively. Peak D has an A_{1g} symmetric graphite lattice vibration mode, which is caused by defects in the graphite lamellae. Peak G is an ideal planar vibration mode of E_{2G} symmetric graphite, which is related to the sp^2 bond carbon atom in the two-dimensional hexagonal graphite layer. Therefore, the intensity

https://doi.org/10.1021/acsomega.1c04318
ACS Omega 2021, 6, 34386−34394

ratio of peaks D and G can measure the degree of carbon defects and graphitization of the sample. The higher the ratio, the more the defects found.[7] These energy bands indicate that both disordered and graphite carbon exist in the carbon material. The wide peak at the D band and the weak peak at 1150 cm^{-1} correspond to the XRD analysis. All activated carbon samples are mainly composed of amorphous carbon. The calculated I_D/I_G of the five samples were 0.9834, 0.9841, 0.9837, 0.97, and 0.9773, indicating that all of the activated carbon samples had a lower graphitization degree (0.52) than commercial activated carbon. In addition, the defects of C_4 were the least, possibly because the lignin fragmentation and purity increased with the increase of NaOH content in the extraction process, and the defect degree of activated carbon reached the minimum value at C_4, as shown in Figure 7.

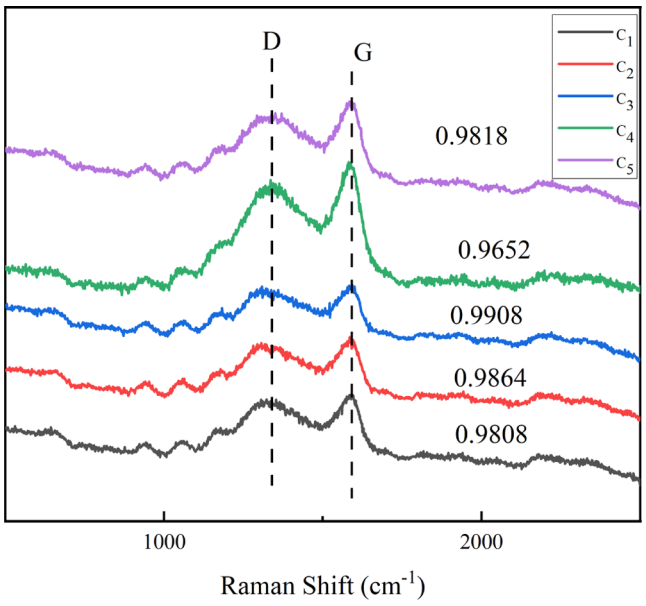

Figure 7. Raman spectra of lignin-based activated carbon.

The adsorption experiment was performed to evaluate the adsorption ability of lignin-based carbon materials in the dark using UV−vis spectroscopy. According to the IUPAC classification, these isotherms belonged to type IV. Furthermore, a rather broad hysteresis loop belonging to type H_2 was observed within a wide range of p/p_0, ascribed to the development of mesoporosity,[31] and failure to close the hysteresis loop indicates the presence of micropores. Similar results are shown in Figure 8B. It can be seen from Figure 8B that the mesoporous size of the product is mainly concentrated to around 2−3 nm. The Brunauer−Emmett−Teller (BET) specific surface area and pore structure of lignin-based activated carbon samples are listed in Table 2.

Lignin is an aromatic macromolecule compound whose heat treatment may produce a mass of volatiles, such as CO, CO_2, and H_2O, leading to more pores, and consequently, the specific surface area was improved.[31] At the stage of gradual increase of NaOH content, namely, AC_1−AC_4, lignin is gradually degraded into small aromatic substances, which is a factor causing the gradual increase of the specific surface area. Consistent with the conclusion discussed above, C_4 has the largest specific surface area (382 $m^2 \cdot g^{-1}$) and also a large pore volume.

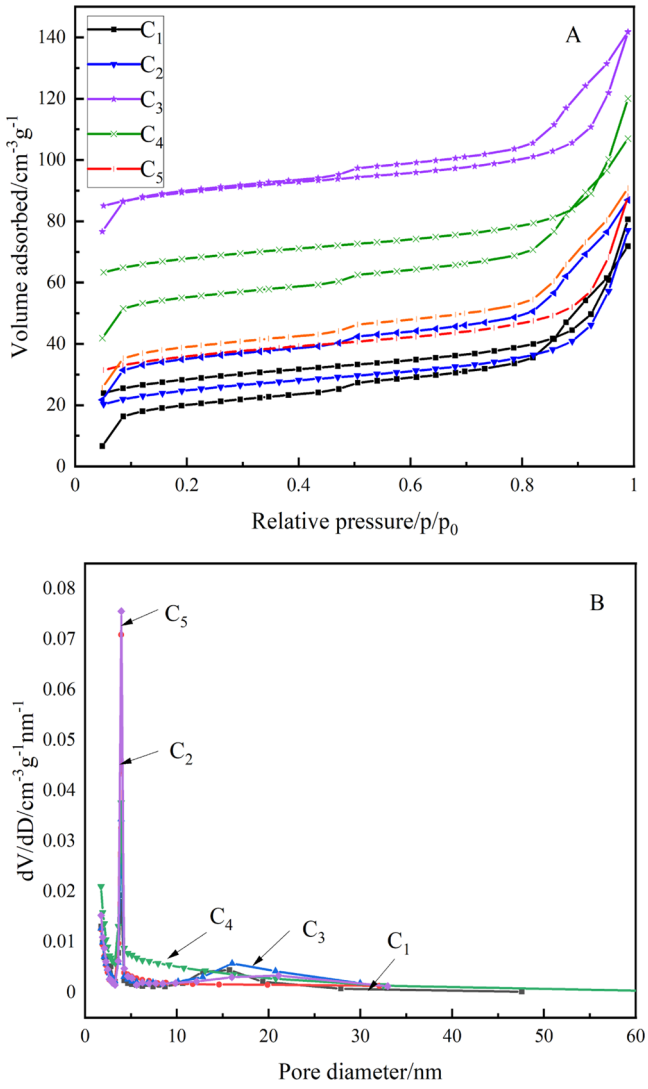

Figure 8. Lignin-based activated carbon. ((A) N_2 adsorption isotherms and (B) pore size distribution curve of lignin-based activated carbon.).

Table 2. Pore Structure Parameters of C_1−C_5

sample	S_{BET} ($m^2 \cdot g^{-1}$)	V_T ($cm^3 \cdot g^{-1}$)	average pore size (nm)	yield (%)
C_1	159.8637	0.115748	2.8962	32.7
C_2	286.8823	0.171855	2.3962	33.5
C_3	277.0314	0.190900	2.7564	34.0
C_4	382.0971	0.257793	2.6987	35.8
C_5	337.3555	0.201500	2.3892	34.9

4. CONCLUSIONS

The effects of alkali and 1,4-butanediol contents on the structure of lignin and lignin activated carbon in the organic solvent process were studied. The results of the first part showed that with the increase of alkali content, the number of ether bonds in lignin decreased, and the number of phenolic hydroxyl groups increased. With the increase of 1,4-butanediol content, the number of lignin ether bonds and phenolic hydroxyl groups decreased because of the formation of C−ONa. During extraction, the increase of alkali and 1,4-butanediol decreased the molecular weight of lignin. The S/G of lignin was negatively correlated with the cross-linking degree, while the LOI was positively correlated with L/C. In

https://doi.org/10.1021/acsomega.1c04318
ACS Omega 2021, 6, 34386−34394

this experimental system, the comprehensive results showed that the optimal conditions for extracting lignin were 60% of 1,4-butanediol per 50 g corn stalk meal and 8 g of NaOH.

In the second part of the experiment, activated carbon samples C_1−C_5 were successfully prepared from lignin AC_1−AC_5, respectively. During lignin extraction, the content of NaOH affects the aromatic results of lignin and subsequently affects the functional groups of activated carbon. The number of phenolic hydroxyl groups in the AC_1−AC_5 samples of lignin was correlated with that of activated carbon samples C_1−C_5. In addition, among a series of activated carbon samples prepared, lignin-based activated carbon C_4 prepared by AC_4 has the minimum defect degree and the maximum specific surface area (382 $m^2 \cdot g^{-1}$).

5. EXPERIMENTAL METHOD

5.1. Extraction of Lignin. In all of the reactions, the solid−liquid ratio was 1:10. Every 50 g of corn stalk powder was reacted with 2, 4, 6, 8, and 10 g of NaOH, which was recorded as AC_1−AC_5, respectively. The contents of 1,4-butanediol in the solution are 0, 30, 60, and 90% (the rest is water), which were recorded as AWR_1−AWR_4, respectively. The experiment was carried out in a 120 °C autoclave for 1 h. After the reaction, the filter cake was washed with 300 mL of distilled water, the filtrate was collected and adjusted to pH 2 with concentrated hydrochloric acid, and then 1200 mL of distilled water was added for water sedimentation. After vacuum filtration and drying, stalk lignin was obtained.

5.2. Preparation of Activated Carbon from Lignin. Lignin AC_1−AC_5 and calcium chloride were mixed in a mass ratio of 1:1.5 and stirred overnight. The mixed slurry was dried completely in an oven at 80 °C. The dried mixture was placed in a pyrolysis furnace and heated to 600 °C at a rate of 5 °C min^{-1} in a nitrogen atmosphere for 2 h. After cooling to room temperature, the material was taken out, washed with 2 M dilute hydrochloric acid for 5 h to remove impurities, filtered with tap water, and dried to obtain lignin-based activated carbon samples, which were recorded as C_1−C_5.

AUTHOR INFORMATION

Corresponding Author

Yong-Shui Qu − *State Key Laboratory of Biochemical Engineering, Institute of Process Engineering, Chinese Academy of Sciences, Beijing 100190, China*; Phone: +86 10 82544852; Email: ysqu@ipe.ac.cn, quyongshui@126.com

Authors

Ying-xia Li − *Beijing University of Chemical Technology, Beijing 100029, China*; orcid.org/0000-0003-0081-5798

Shao-xing Hou − *Beijing University of Chemical Technology, Beijing 100029, China; State Key Laboratory of Biochemical Engineering, Institute of Process Engineering, Chinese Academy of Sciences, Beijing 100190, China*; orcid.org/0000-0003-1525-986X

Quan-yuan Wei − *Beijing Zhong Yuan Chuang Neng Engineering and Technology, Ltd., Beijing 100101, China; Beijing International Cooperation Base in Sci-tec Innovation of Organic Waste Treatment, Beijing 100101, China*

Xiao-shan Ma − *Beijing University of Chemical Technology, Beijing 100029, China; State Key Laboratory of Biochemical Engineering, Institute of Process Engineering, Chinese Academy of Sciences, Beijing 100190, China*

Complete contact information is available at: https://pubs.acs.org/10.1021/acsomega.1c04318

Notes

The authors declare no competing financial interest.

ACKNOWLEDGMENTS

This work was supported by the following foundations: National Science and Technology Major Project of the Ministry of Science and Technology of China (No. 2018ZX07105-004), National Natural Science Foundation of China (No. 2170060476), and Beijing Science and Technology Plan (No. Z181100002418019).

REFERENCES

(1) Sahoo, S.; Seydibeyoğl, M. Ö.; Mohanty, A. K.; Misra, M. Mohanty Characterization of industrial lignins for their utilization in future value added applications. *Biomass Bioenergy* **2011**, *35*, 4230−4237.

(2) Cao, Y.; Zhang, C.; Tsang, D. C. W.; Fan, J.; Clark, J. H.; Zhang, S. Hydrothermal Liquefaction of Lignin to Aromatic Chemicals: Impact of Lignin Structure. *Ind. Eng. Chem. Res.* **2020**, *59*, 16957−16969.

(3) Kumar, A.; Anushree; Kumar, J.; Bhaskar, T. Utilization of lignin: A sustainable and eco-friendly approach. *J. Energy Inst.* **2020**, *93*, 235−271.

(4) Bajwa, D. S.; Pourhashem, G.; Ullah, A. H.; Bajwa, S. G. A concise review of current lignin production, applications, products and their environmental impact. *Ind. Crops Prod.* **2019**, *139*, No. 111526.

(5) Liu, X.; Z, M.; Wang, J.; et al. Chemical Structure of Bioethanol Lignin by Low-Temperature Alkaline Catalytic Hydrothermal Treatment. *Spectrosc. Spectral Anal.* **2013**, *33*, 2940−2944.

(6) Zhu, Y.; Li, Z.; Chen, J. Applications of lignin-derived catalysts for green synthesis. *Green Energy Environ.* **2019**, *4*, 210−244.

(7) Gezahegn, S.; Garcia, C.; Lai, R.; Zhou, X.; Tjong, J.; Thomas, S. C.; Huang, F.; Jaffer, S.; Weimin, Y.; Sain, M. Benign species-tuned biomass carbonization to nano-layered graphite for EMI filtering and greener energy storage functions. *Renewable Energy* **2021**, *164*, 1039−1051.

(8) Li, M.; Li, Y. W.; Cai, Q. Y.; Zhou, S. Q.; Mo, C. H. Spraying carbon powder derived from mango wood biomass as high-performance anode in bio-electrochemical system. *Bioresour. Technol.* **2020**, *300*, No. 122623.

(9) Chang, Z.; Dai, J.; Xie, A.; He, J.; Zhang, R.; Tian, S.; Yan, Y.; Li, C.; Xu, W.; Shao, R. From Lignin to Three-Dimensional Interconnected Hierarchically Porous Carbon with High Surface Area for Fast and Superhigh-Efficiency Adsorption of Sulfamethazine. *Ind. Eng. Chem. Res.* **2017**, *56*, 9367−9375.

(10) Klose, M.; Reinhold, R.; Logsch, F.; Wolke, F.; Linnemann, J.; Stoeck, U.; Oswald, S.; Uhlemann, M.; Balach, J.; Markowski, J.; Ay, P.; Giebeler, L. Softwood Lignin as a Sustainable Feedstock for Porous Carbons as Active Material for Supercapacitors Using an Ionic Liquid Electrolyte. *ACS Sustainable Chem. Eng.* **2017**, *5*, 4094−4102.

(11) Serna-Loaiza, S.; Zikeli, F.; Adamcyk, J.; Friedl, A. Towards a wheat straw biorefinery: Combination of Organosolv and Liquid Hot Water for the improved hydrolysis of lignin and hemicellulose. *Bioresour. Technol. Rep.* **2021**, *14*, No. 100667.

(12) Wang, K.; Feng, X.; Sun, R. Molecular Characteristics of Kraft-AQ Pulping Lignin Fractionated by Sequential Organic Solvent Extraction. *Int. J. Mol. Sci.* **2010**, *11*, 2988.

(13) Zhang, H.; Bai, Y.; Yu, B.; Liu, X.; Chen, F. A practicable process for lignin color reduction: fractionation of lignin using methanol/water as a solvent. *Green Chem.* **2017**, *19*, 5152−5162.

(14) Huang, T.; Cheng, K. H.; Wang, C. H. Effects of Tween-80 and Alkali Pretreatment on the Content of Lignin of Straw and Enzymatic Hydrolysis. *J. Cellul. Sci. Technol.* **2011**, *19*, 52−58.

(15) Hu, J.; Liu, Y.; Shi, R. Study on Lignin Carbonization with Its Application. *Hans J. Chem. Eng. Technol.* **2015**, *05*, 53−58.
(16) Martínez, M. L.; Torres, M. M.; Guzmán, C.; Maestri, D. M. Preparation and characteristics of activated carbon from olive stones and walnut shells. *Ind. Crops Prod.* **2006**, *23*, 23−28.
(17) Liou, T. H.; Wu, S. J. Characteristics of microporous/mesoporous carbons prepared from rice husk under base- and acid-treated conditions. *J. Hazard. Mater.* **2009**, *171*, 693−703.
(18) Aygün, A.; Yenisoy-Karaka, S.; Duman, I. Production of granular activated carbon from fruit stones and nutshells and evaluation of their physical, chemical and adsorption properties. *Microporous Mesoporous Mater.* **2003**, *66*, 189−195.
(19) Song, X.; Zhang, Y.; Chang, C. Novel Method for Preparing Activated Carbons with High Specific Surface Area from Rice Husk. *Ind. Eng. Chem. Res.* **2012**, *51*, 15075−15081.
(20) Liu, J.; Deng, Y.; Li, X.; Wang, L. Promising Nitrogen-Rich Porous Carbons Derived from One-Step Calcium Chloride Activation of Biomass-Based Waste for High Performance Supercapacitors. *ACS Sustainable Chem. Eng.* **2016**, *4*, 177−187.
(21) Sui, X. J.; Wu, S. B. Study on Mechanism of Action of Catalysts on Liquefaction of Bagasse Alkali Lignin. *Adv. Mater. Res.* **2011**, *383*−*390*, 6145−6150.
(22) Gierer, J.; Lenz, B.; Noren, I.; Soederberg, S. Reactions of lignin during dulfate cooking. III. The splitting of aryl-alkyl ether bonds in milled wood lignin by alkali. *Tappi J.* **1964**, *47*, 233−239.
(23) Wang J, J. E.; Zhao, N. Research progress of biomass carbon-materials by hydrothermal process. *Shanxi Archit.* **2014**, 140−141.
(24) Gominho, J.; Costa, R.; Loureno, A.; Neiva, D. M.; Pereira, H. The effect of different pre-treatments to improve delignification of eucalypt stumps in a biorefinery context. *Bioresour. Technol. Rep.* **2019**, *6*, 89−95.
(25) Auxenfans, T.; Cronier, D.; Chabbert, B.; Paes, G. Understanding the structural and chemical changes of plant biomass following steam explosion pretreatment. *Biotechnol Biofuels* **2017**, *10*, No. 36.
(26) Pooja, N. S.; Padmaja, G. Enhancing the Enzymatic Saccharification of Agricultural and Processing Residues of Cassava through Pretreatment Techniques. *Waste Biomass Valorization* **2015**, *6*, 303−315.
(27) Taheri, H.; Samyn, P. Effect of homogenization (micro-fluidization) process parameters in mechanical production of micro- and nanofibrillated cellulose on its rheological and morphological properties. *Cellulose* **2016**, *23*, 1221−1238.
(28) Rowlandson, J. L.; Edler, K. J.; Tian, M.; Ting, V. P. Toward Process-Resilient Lignin-Derived Activated Carbons for Hydrogen Storage Applications. *ACS Sustainable Chem. Eng.* **2020**, *8*, 2186−2195.
(29) Wang, S. J.; et al. Production of activated carbon from corn cob by calcium chloride activation method. *Window Pract. Tech.* **1995**, 4−5.
(30) Perezdrienko, I. V.; Molodozhenyuk, T. B.; Shermatov, B. E.; Yunusov, M. P. Effect of Carbonization Temperature and Activation on Structural Formation of Active Lignin Carbons. *Russ. J. Appl. Chem.* **2001**, *74*, 1650−1652.
(31) Gang, X.; Rongbing, W.; Huilong, Z.; Mingjiang, N.; Xiang, G.; Kefa, C. Preparation and Characterization of Activated Carbons Based Alkali Lignin by KOH Chemical Activation. *J. Combust. Sci. Technol.* **2014**, *20*, 14−20.

https://doi.org/10.1021/acsomega.1c04318
ACS Omega 2021, 6, 34386−34394